

*Simultaneous measurement of the  $^{233}\text{U}$   
capture and fission cross section using the  
Calorimetric Shape Decomposition method*

**Carlos Carrapiço and the n\_TOF Collaboration**

**Presented at**

**Wonder 2012 Aix-en-Provence**

**25 September**

# Motivation

The Thorium-Uranium (Th-U) fuel cycle has been envisaged as an alternative to the Uranium-Plutonium (U-Pu) fuel cycle for electricity generation using nuclear power reactors.

- Natural abundance of Thorium
- Improved proliferation resistance relative to the U-Pu fuel cycle
- Better neutronics performance throughout the whole neutron energy range compared to the U-Pu fuel
- Lower radiotoxicity of the generated spent fuel
- Better economics and public acceptance compared to those using the U-Pu fuel cycle (prior to the Generation IV nuclear reactors).

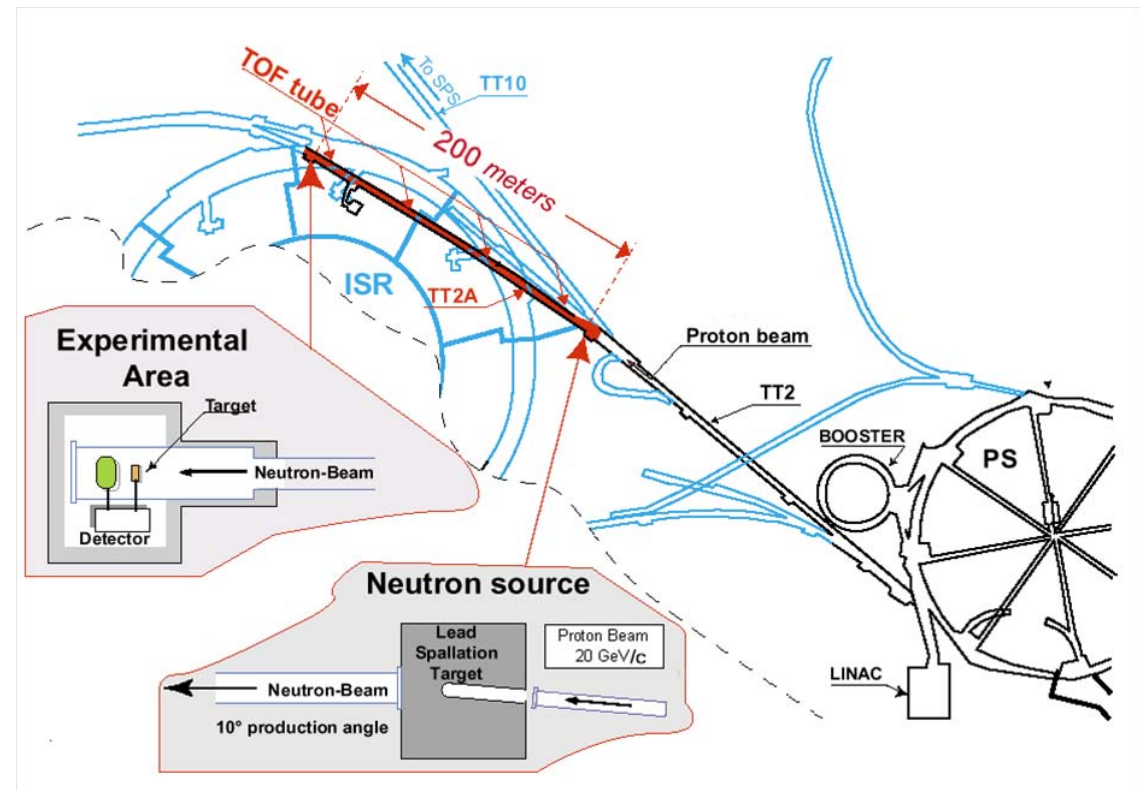
In a nuclear reactor operated using the Th-U fuel cycle,  $^{233}\text{U}$  is a key nuclide governing the neutronics performance of the system and consequently its economics, nuclear safety and proliferation resistance properties and characteristics.

# The n\_TOF facility

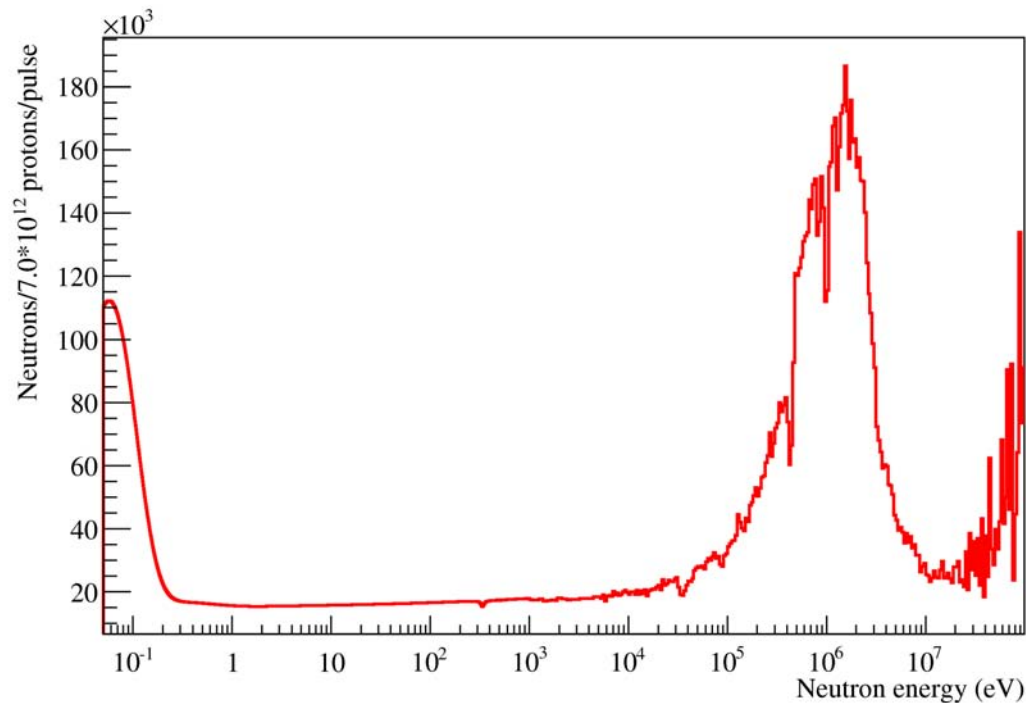
Neutrons in the wide energy range from thermal to approximately 1 GeV are generated via spallation reactions triggered by 20 GeV/c protons impinging on a lead spallation target.

The proton beam is characterized by a momentum of 20 GeV/c in a bunch of  $7 \times 10^{12}$  protons with a 7 ns pulse width.

- Very high instantaneous flux of neutron per burst
- Low duty cycle
- Excellent neutron energy resolution, flight path with 185m and  $\Delta E/E = 0.01$  (10eV) or 0.0005 (10keV)
- Low background
- Fast electronics and Data Acquisition System (DAQ)



# The n\_TOF facility

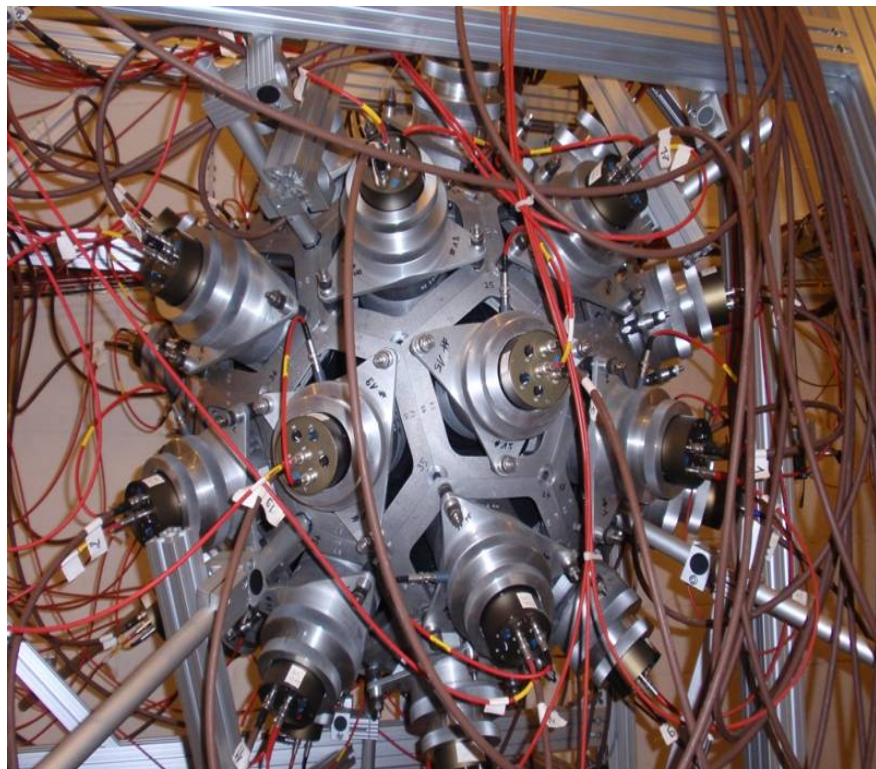


The neutron fluence assessment was performed using:

- ✓ Two calibrated fission chambers from Physikalisch-Technische Bundesanstalt (PTB)
- ✓ Silicon detector associated with a <sup>6</sup>Li foil
- ✓ C<sub>6</sub>D<sub>6</sub> detectors
- ✓ Parallel Plate Avalanche Chambers (PPAC).

In the experimental area a total of  $8.0 \cdot 10^5$  Neutrons/proton pulse between 1 - 10<sup>8</sup> eV are available to measure neutron induced cross sections

# The detection system and sample



- **A Total Abortion Calorimeter (TAC)** composed of 40 barium fluoride crystal
- **95% solid angle** and **~100% detection efficiency** of a capture event

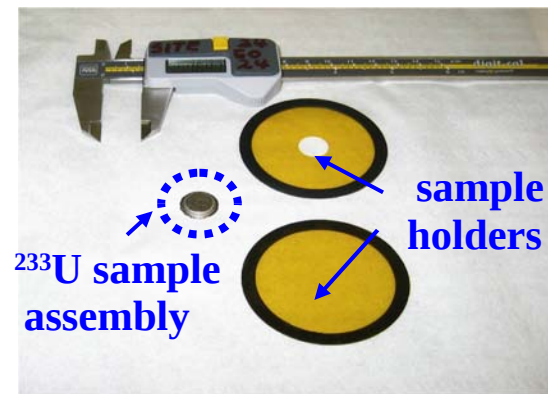
Isotopic composition:

$^{233}\text{U}$  99.01%

$^{234}\text{U}$  0.74%

$^{235}\text{U}$  0.22%

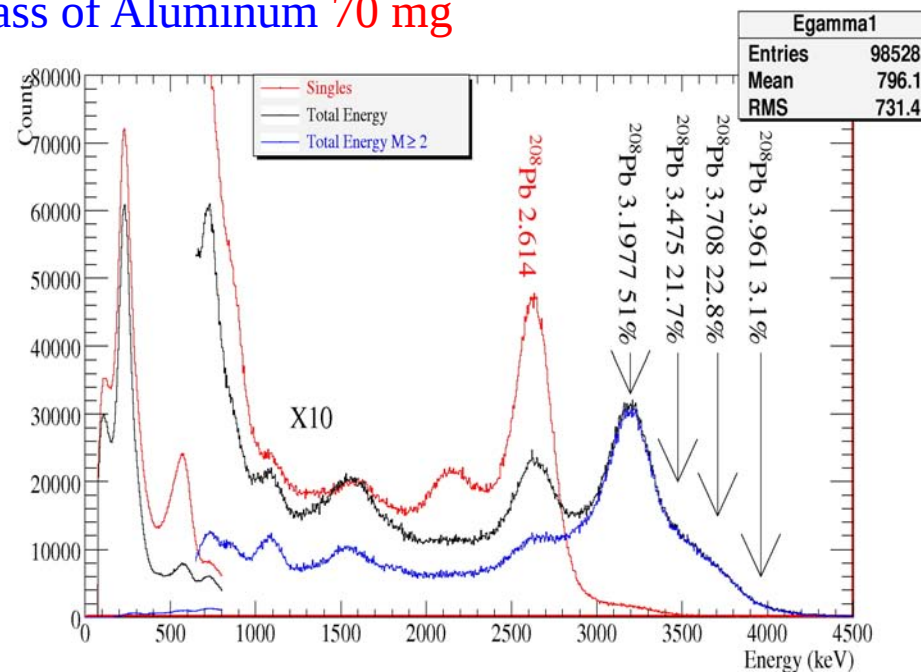
$^{238}\text{U}$  0.03%



Mass of  $^{233}\text{U}$  91 mg

Mass of Titanium 277.1 mg

Mass of Aluminum 70 mg

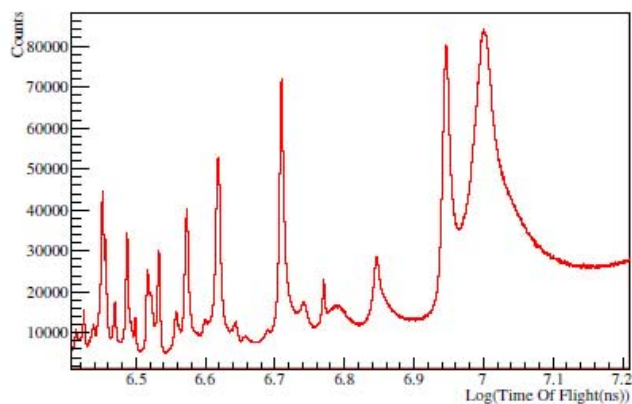
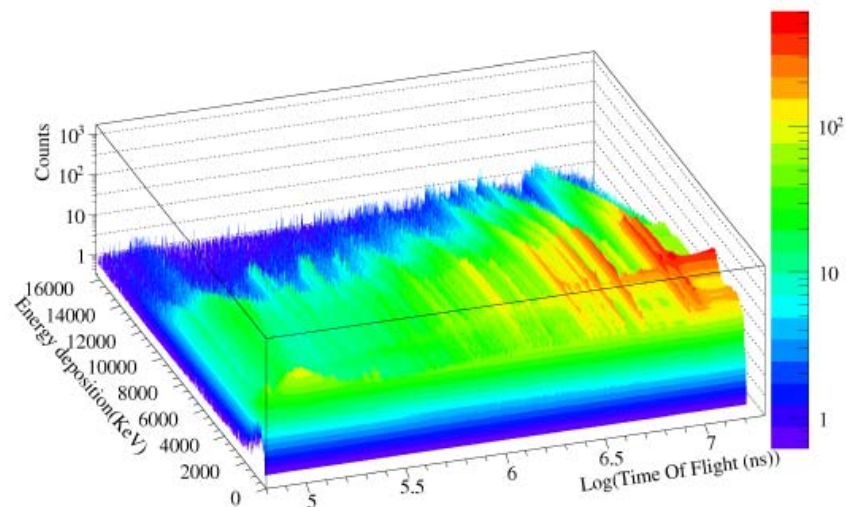


Measured sample related activity (0.356 MBq)

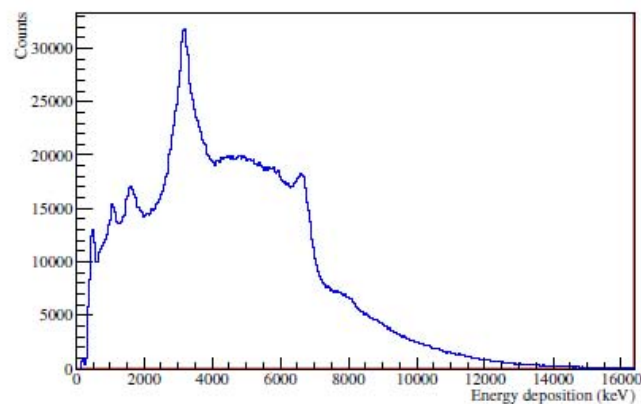


# The $^{233}\text{U}$ data analysis

Projections  
with conditions



Time-of-flight

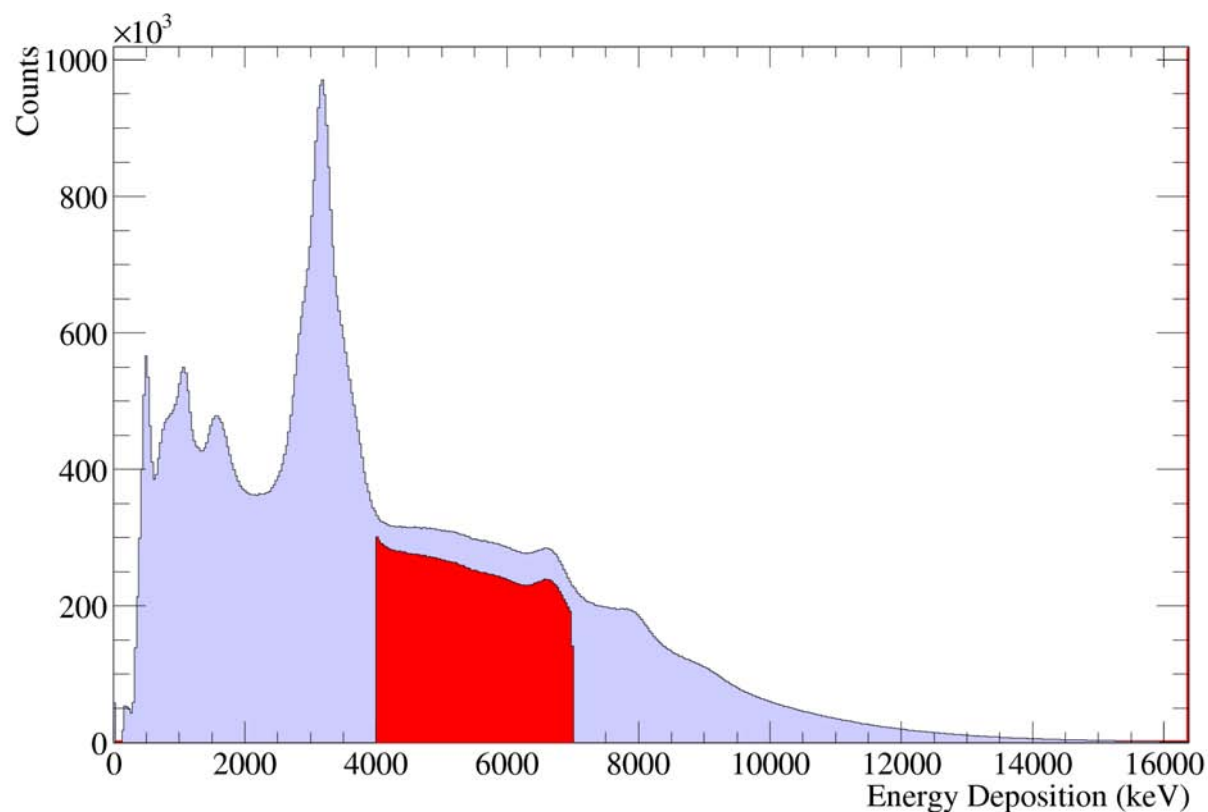


Energy deposition

# Assessing the $^{233}\text{U}$ cross sections

## The problem

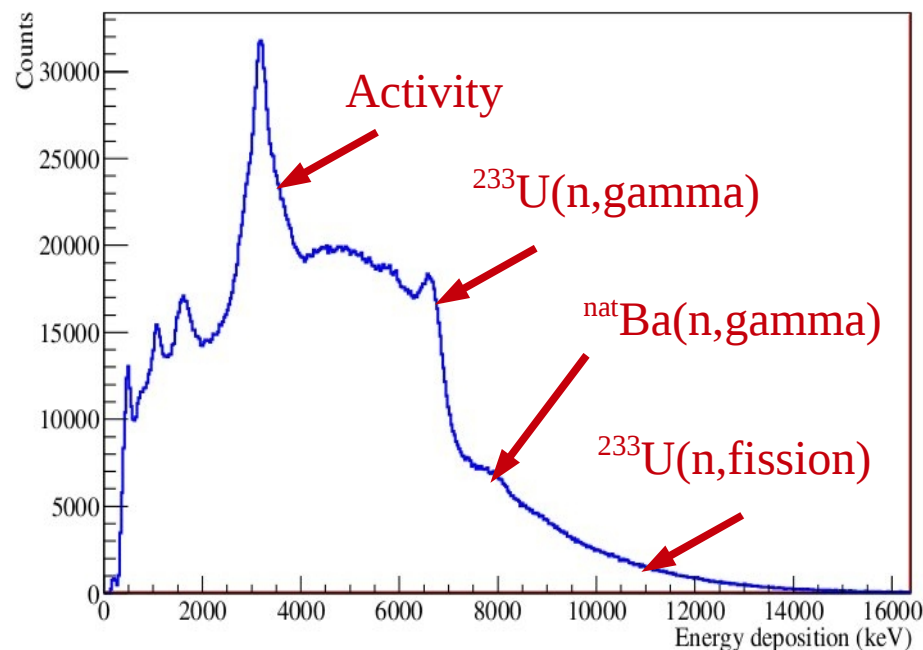
	Low Edep keV	High Edep keV	Average Edep keV	Low Mult	High Mult	Average Mult
Capture	300	6900	4630	2	6	3.69
Fission	300	16000	4955	2	20	5.5



The discrimination between capture and fission is not possible with an analysis based on applying selection criteria in multiplicity and total energy deposition

# Calorimetric Shape Decomposition

## Concept



- Using the CSD method, the contributions of the different reactions are discriminated solely by the TAC energy response to each reaction, independent of selection criteria. It requires to know the open reaction channels and the respective energy deposition spectra.

The following assumptions must be verified for the CSD method to work:

- ✓ The TAC energy response to capture and fission is assumed to be neutron energy independent. The large intrinsic efficiency of the TAC makes the total energy deposition highly independent from the electromagnetic deexcitation pattern.
- ✓ The coincidence time window is small enough to avoid the addition of different contributions. Summing due to the coincidence window and Pile-up in each individual crystal ( $<1.2$  counts/ $\mu$ s at 1 keV and  $<0.7$  counts/ $\mu$ s below 100 eV ).
- ✓ The shape of each contribution is linear independent from the others and the total energy deposition spectrum can be expressed as a linear combination of the individual contributions.

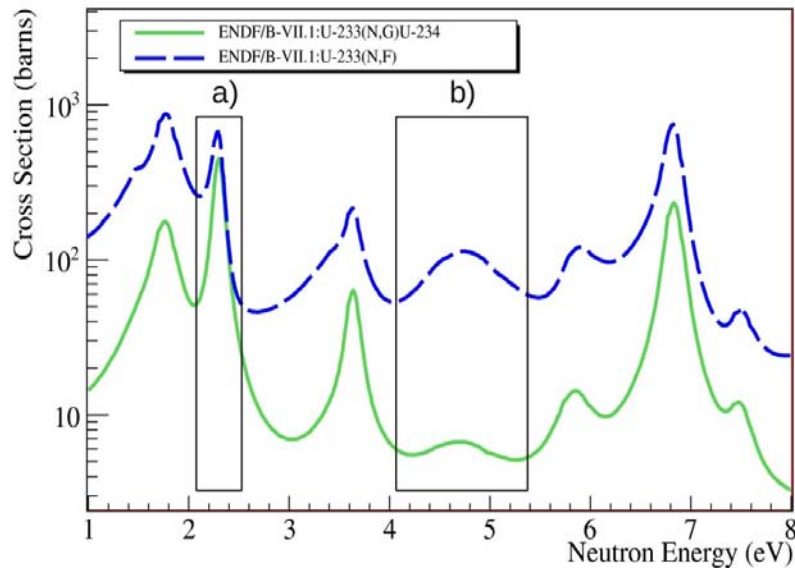
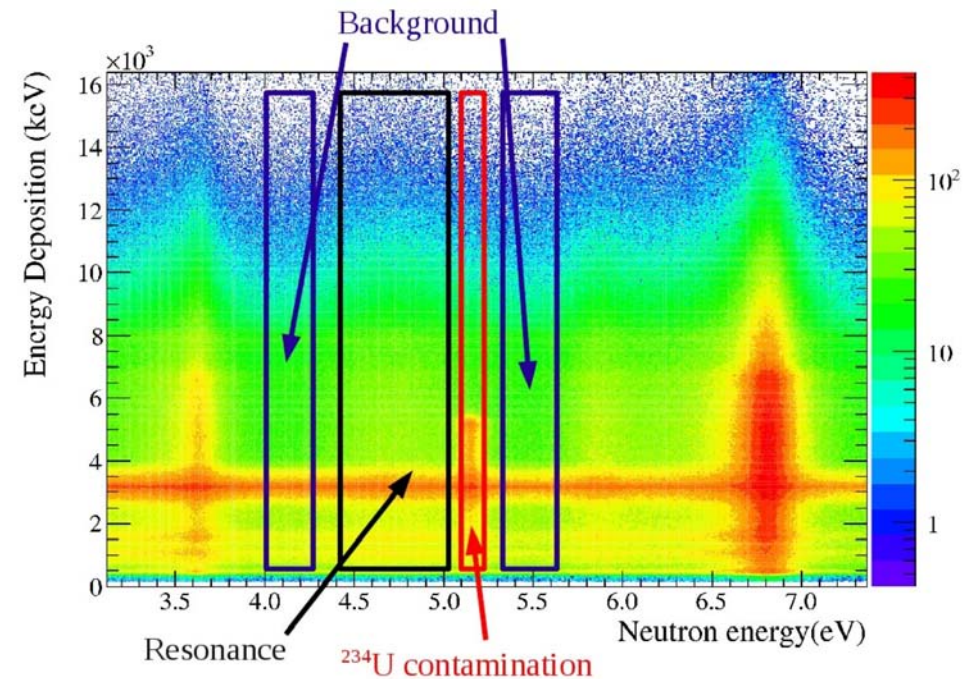
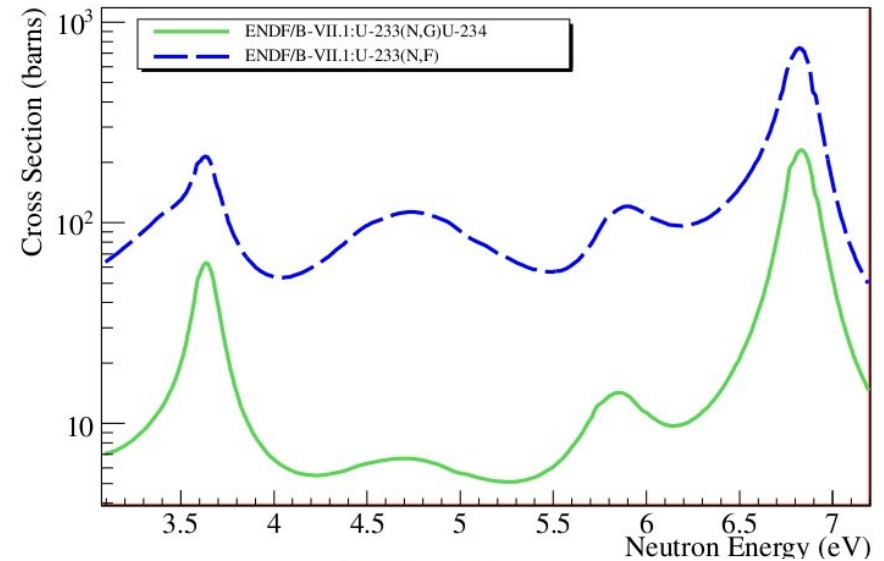


# TAC response to Fission

To obtain the characteristic TAC energy response for each reaction, it is necessary to measure it alone or with a set of conditions that allows the discrimination.

The main difficulty rests in the neutron capture and neutron induced fission events.

## Calorimetric Shape Decomposition



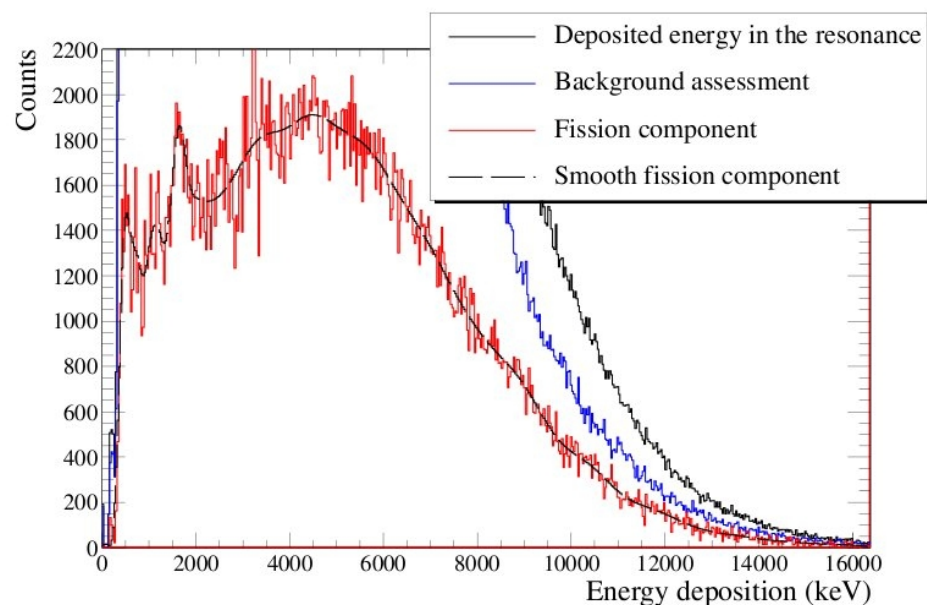
a) At 2.28 eV the ratio between capture and fission is 1

b) At 4.5 eV the cross section is dominated by fission.

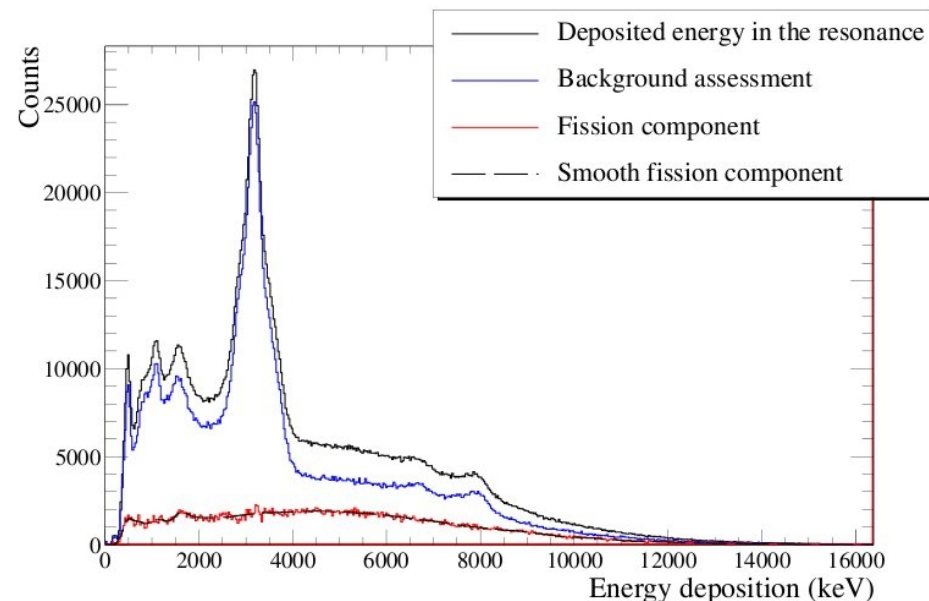
# TAC response to Fission

To determine the TAC energy response to fission, the energy deposition pattern in the 4.5 eV resonance and in the surrounding gaps between the neighboring resonances have been analyzed.

The counts in the resonance are due to fission events, superimposed by time-independent background from the sample related activity and other uncorrelated backgrounds.



## Calorimetric Shape Decomposition



It should be stressed that in the energy range of interest, the effect of sample-scattered neutrons belongs to this time-independent component.

This component is assessed in the regions outside the resonance, where the fission contribution is less important and the non-resonant contributions are dominating the data.

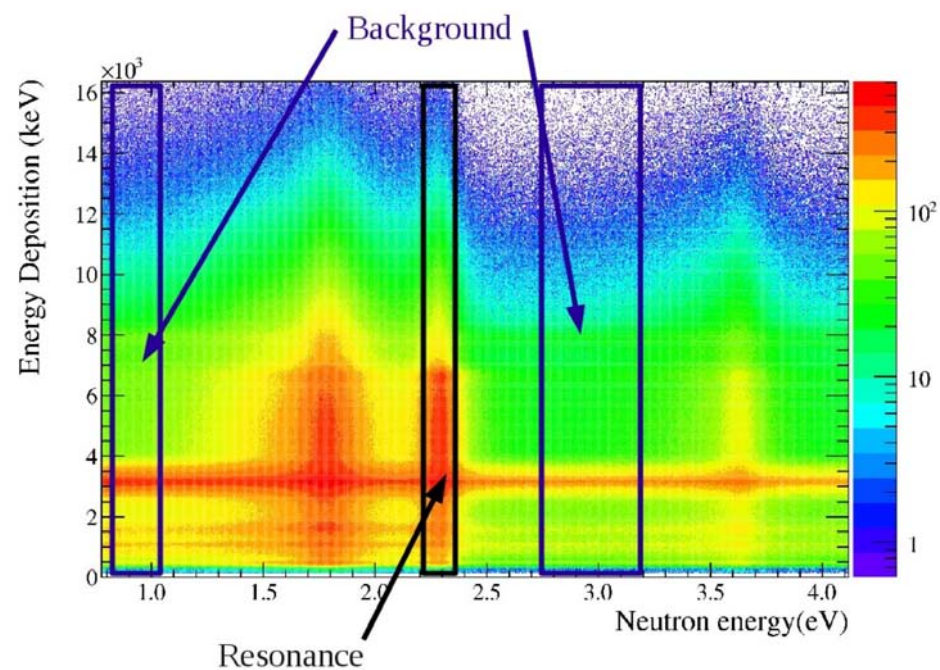
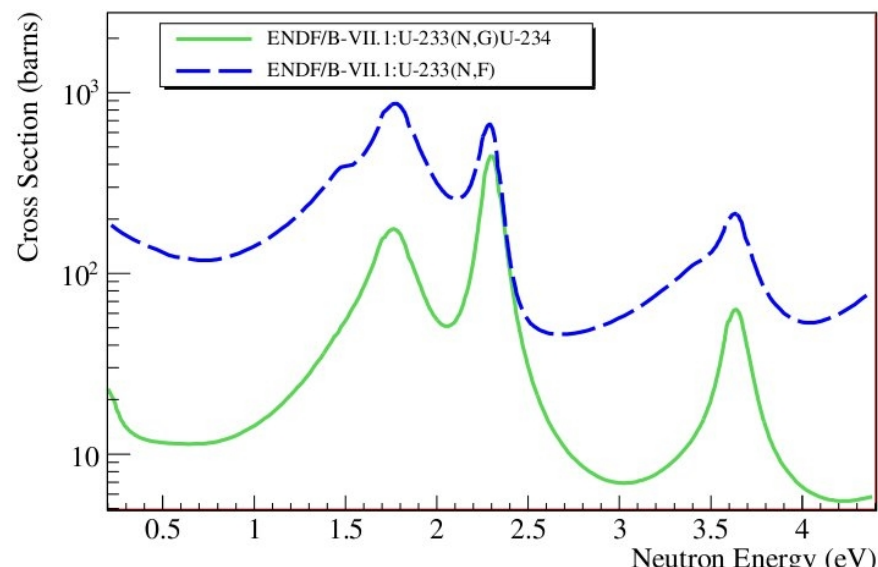
# TAC response to Capture

The energy response of the TAC to neutron capture events was assessed in the 2.28 eV resonance.

The capture-to-fission ratio of that resonance is close to one, much higher than the average of the resolved resonance region, which is typically a factor of 10 lower.

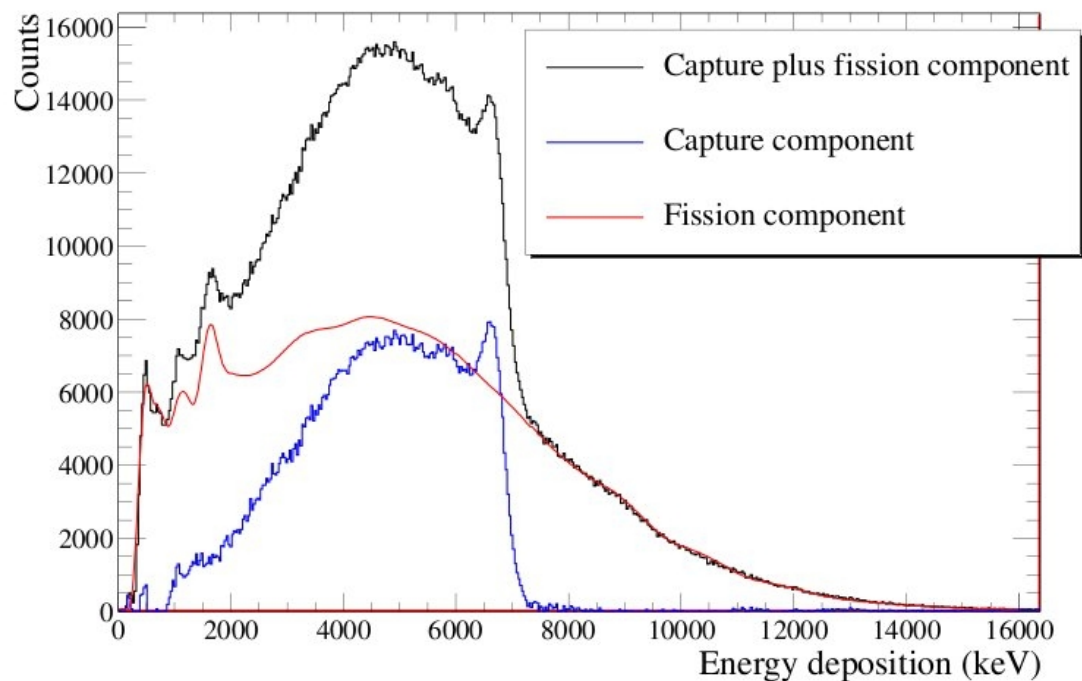
The capture and fission components have been separated using the same background subtraction as for the 4.5 eV resonance

## Calorimetric Shape Decomposition



# TAC response to Capture

## Calorimetric Shape Decomposition

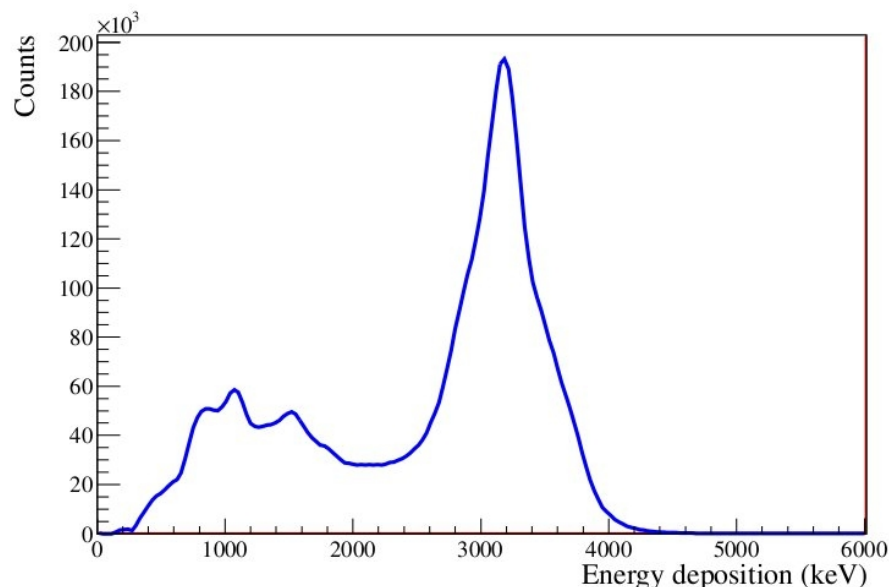


The correction for the fission component was obtained by a linear fit of the fission distribution above the neutron binding energy of  $^{233}\text{U}$  of 6.9 MeV, where all counts could be considered as fission events.



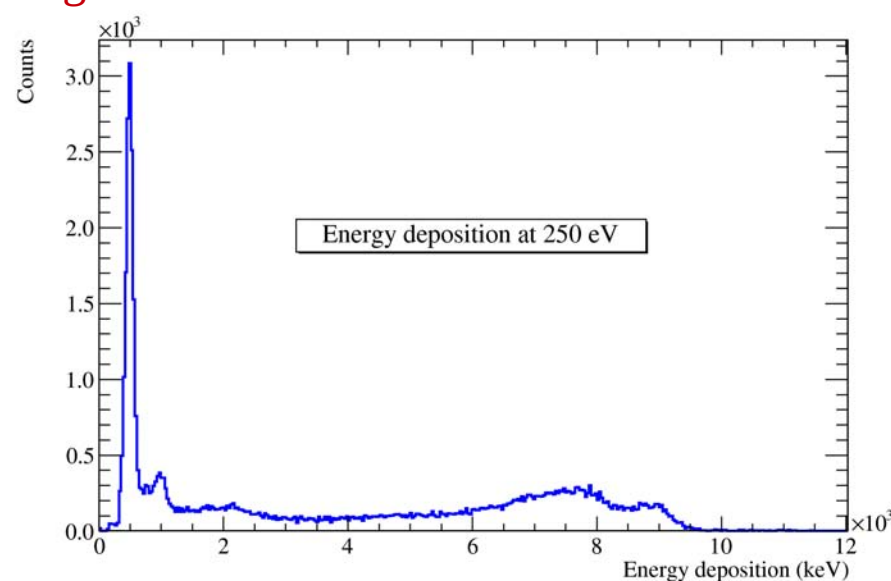
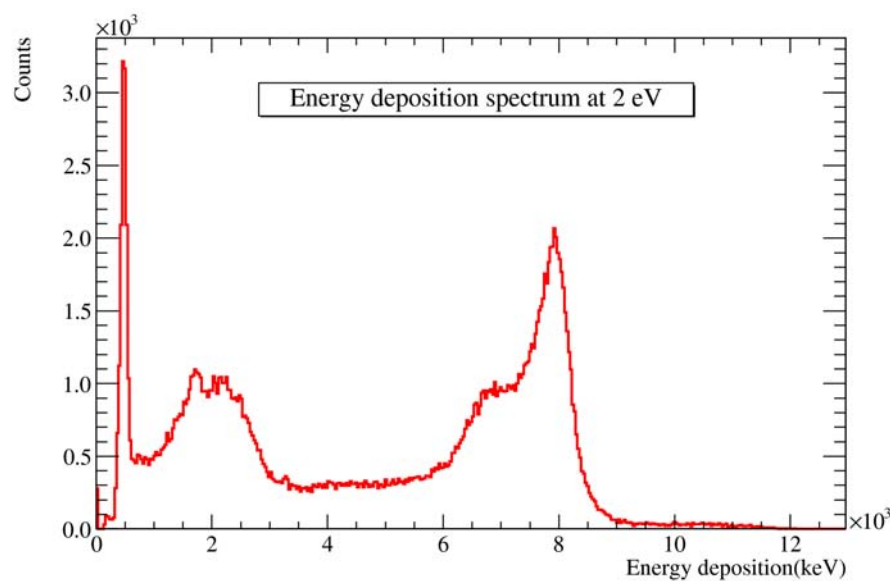
# TAC response to sample related activity and to neutron scattering in the canning

## Calorimetric Shape Decomposition



The TAC response to the sample related activity is neutron energy independent.

- On the contrary, the TAC response to neutron scattering in the canning is dependent on the neutron energy.
- The respective contributions have been determined for each TOF bin directly by the measured TAC energy response of a titanium canning with a blank aluminum backing.



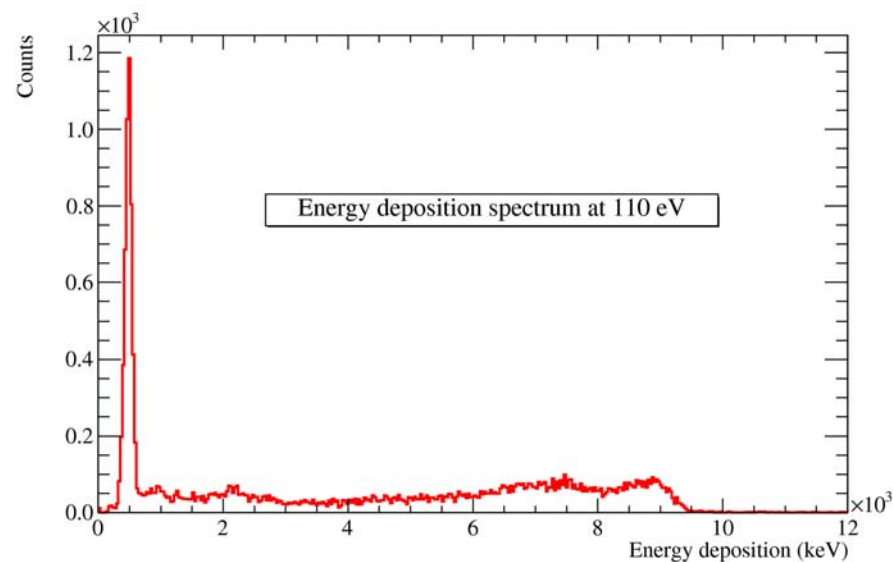
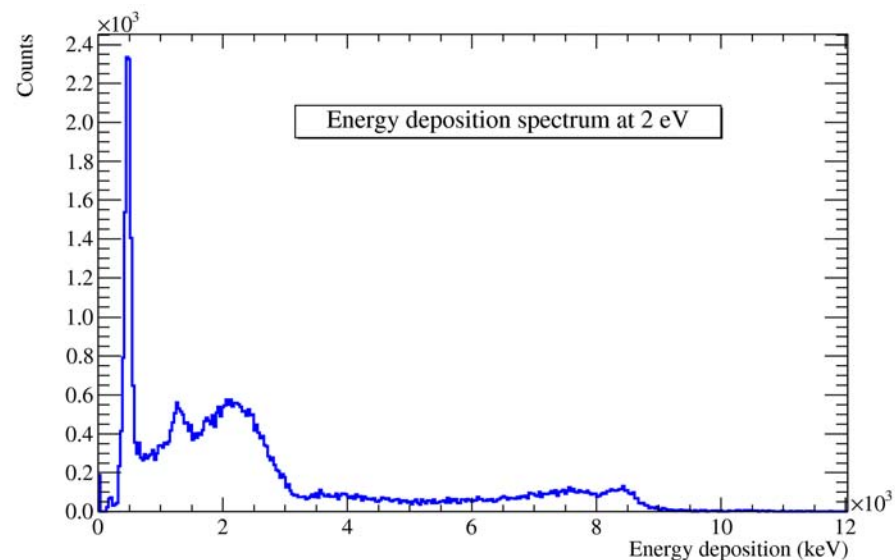


# TAC response to neutron scattering in the $^{233}\text{U}$ mass

## Calorimetric Shape Decomposition

The contribution of neutron scattering from the  $^{233}\text{U}$  had to be inferred from a background run with a carbon sample.

Carbon can be considered as a pure scatterer, which was assumed to simulate the scattering effect of  $^{233}\text{U}$ .



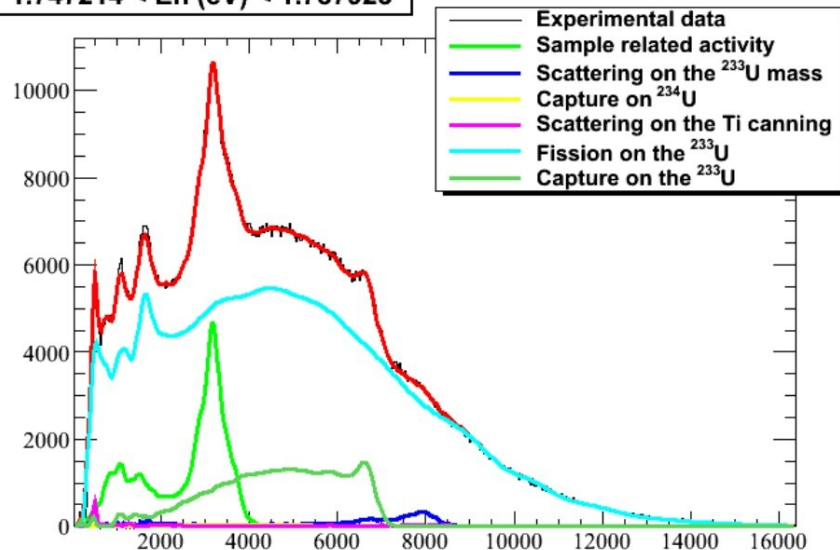
This approximation is justified because it turned out that  $^{12}\text{C}$  exhibits the same TAC signature for scattered neutrons as  $^{233}\text{U}$ .

The neutron scattering is detected via the gammas produced due to the interaction of the scattered neutrons in the structural materials of the detection systems.

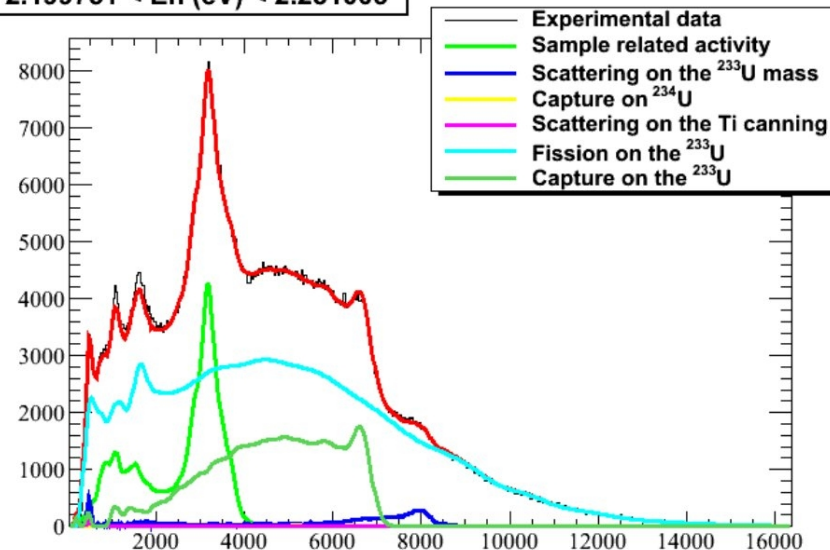
# Yield Assessment: CSD method

$$S_{total} = \alpha(E_n) \cdot S_{capture} + \beta(E_n) \cdot S_{fission} + \gamma(E_n) \cdot S_{activity} + \delta(E_n) \cdot S_{canning} + \epsilon(E_n) \cdot S_{^{233}\text{U} \text{ scattering}}$$

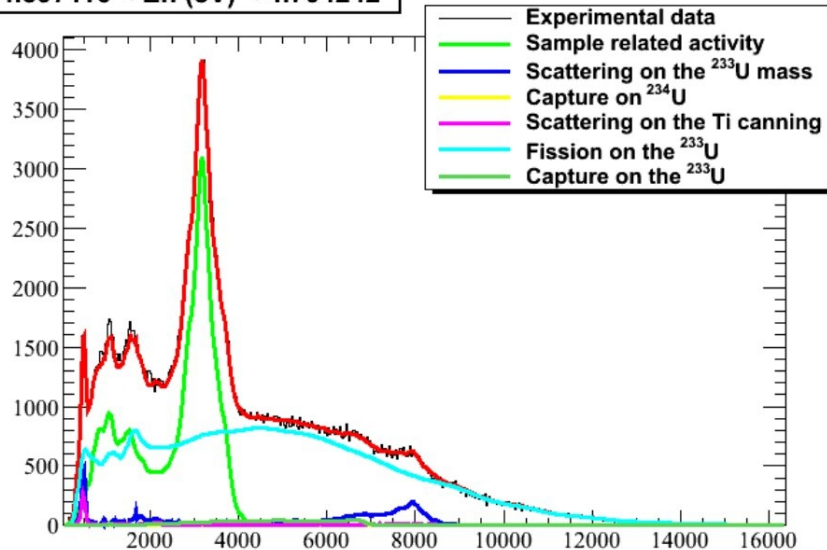
1.747214 < En (eV) < 1.787923



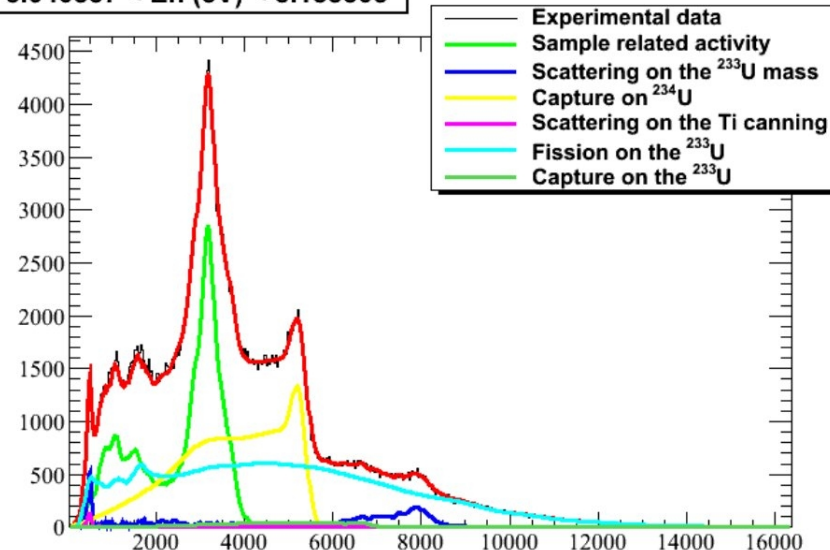
2.199751 < En (eV) < 2.251005



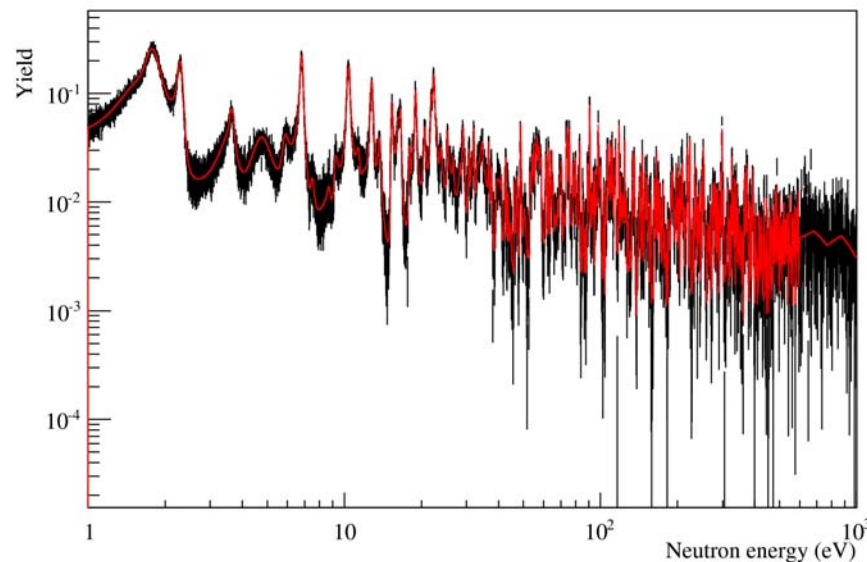
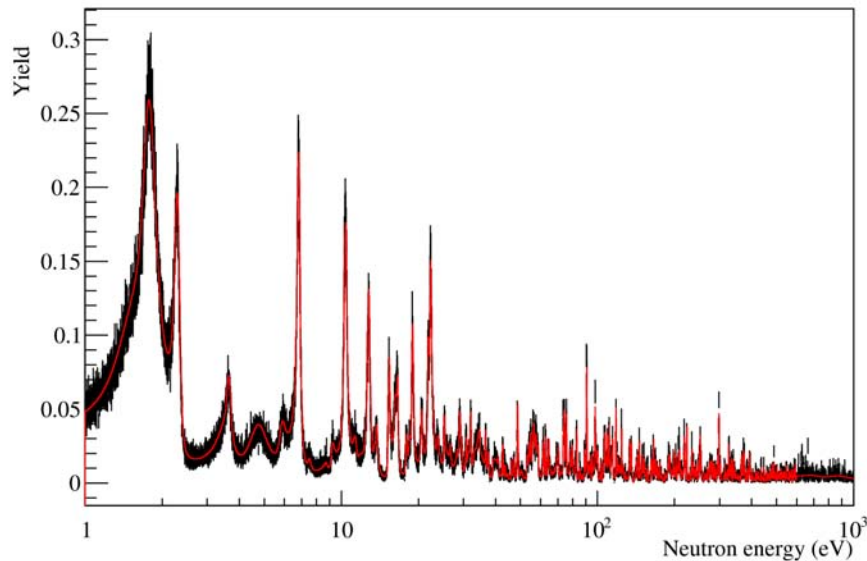
4.597116 < En (eV) < 4.704242



5.040837 < En (eV) < 5.158305



# Results: Fission Yield

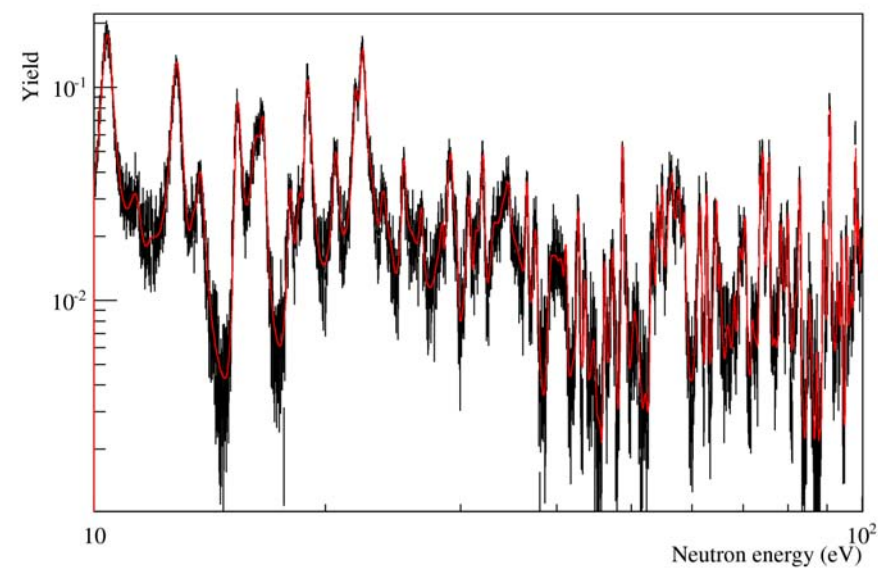
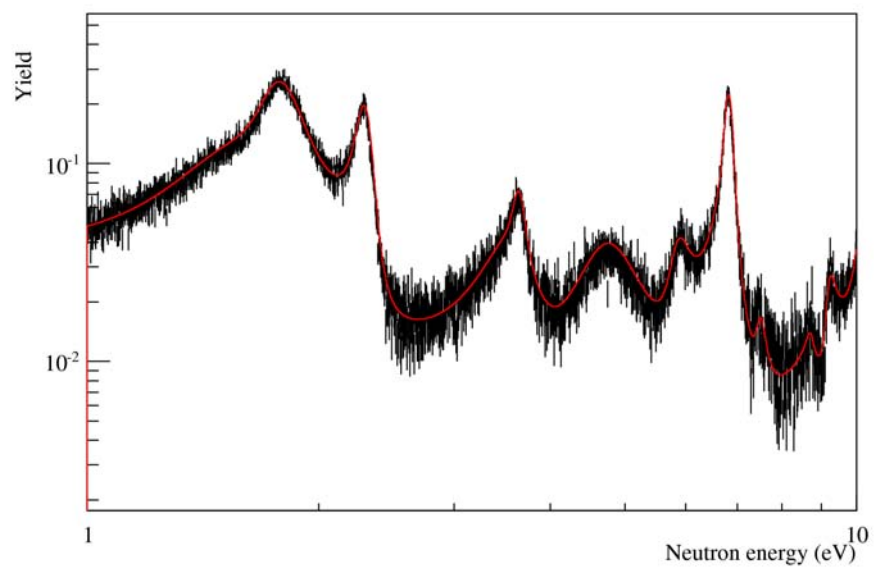
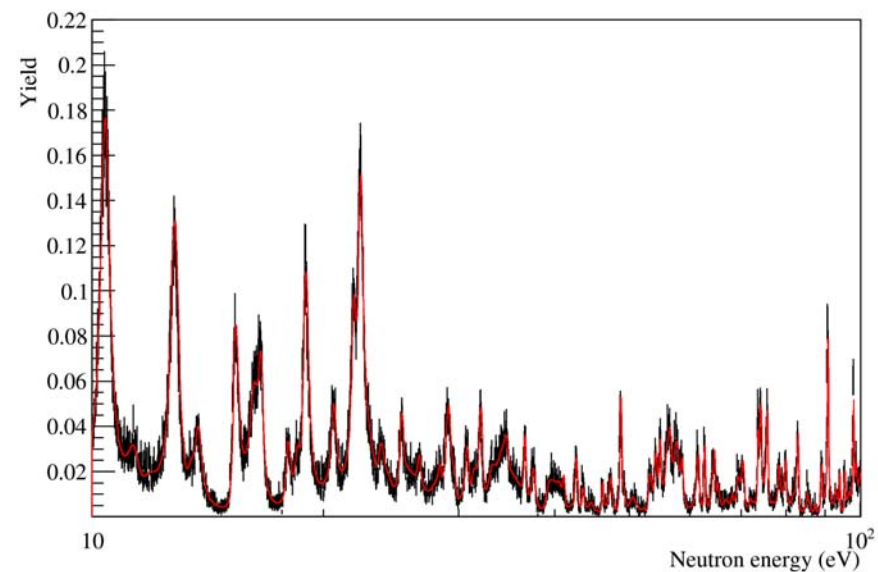
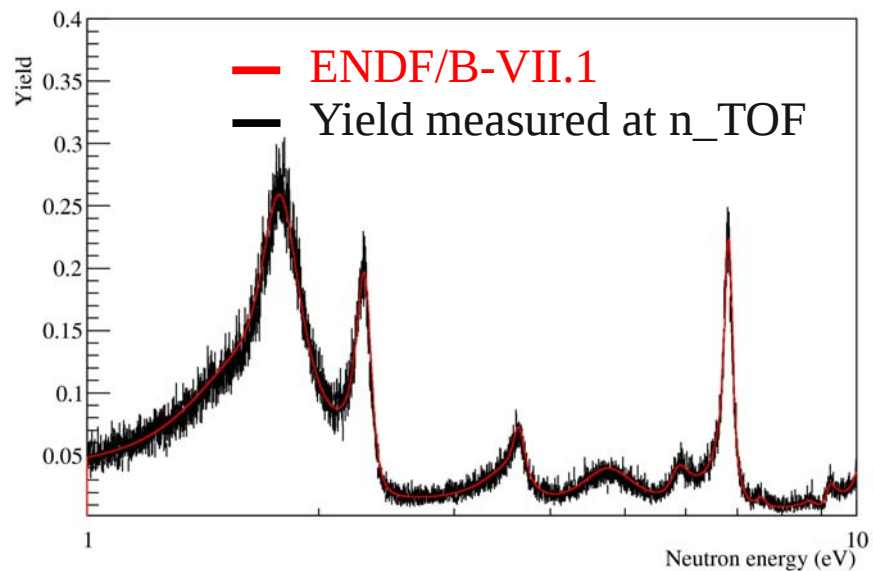


The neutron induced fission yield assessment for the  $^{233}\text{U}$  using the n\_TOF experimental data is compared with the data from the ENDF/B-VII.1 library and shows a good agreement.

The agreement in normalization and shape, validates the CSD method to decompose the total energy deposition spectrum and discriminate between competing reactions and also the Monte Carlo study performed to understand the TAC's response to the prompt gamma radiation emitted in fission events.

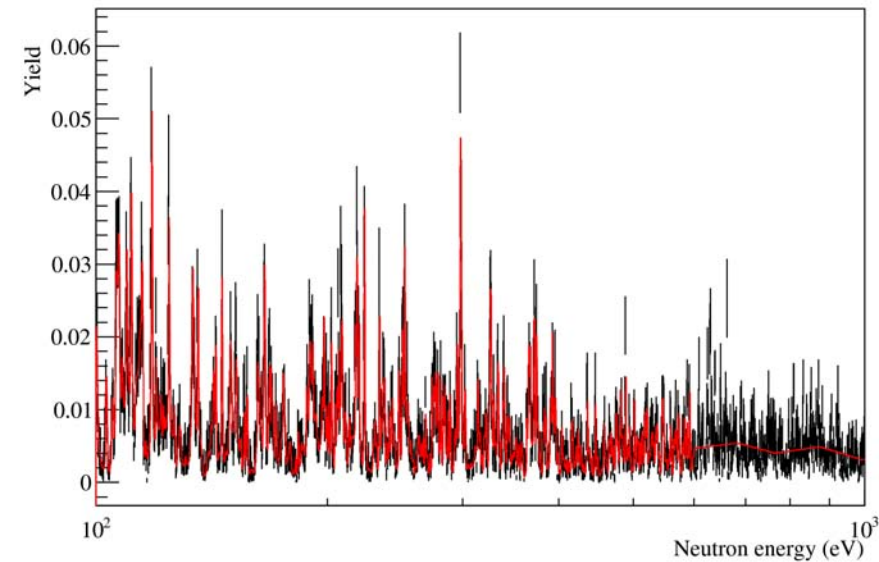
— ENDF/B-VII.1  
— Yield measured at n\_TOF

# Results: Fission Yield



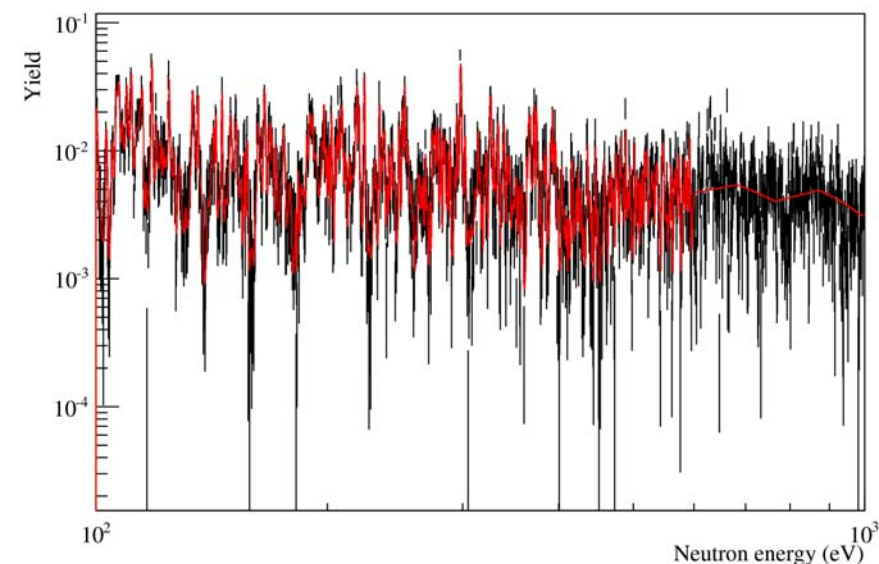


# Results: Fission Yield



Above the resolved resonance region (which extends until 600 eV), the data taken in n TOF shows a number of structures.

A resonance analysis will be attempted in this region but the overlap between resonances may lead to the impossibility of discriminate between resonances

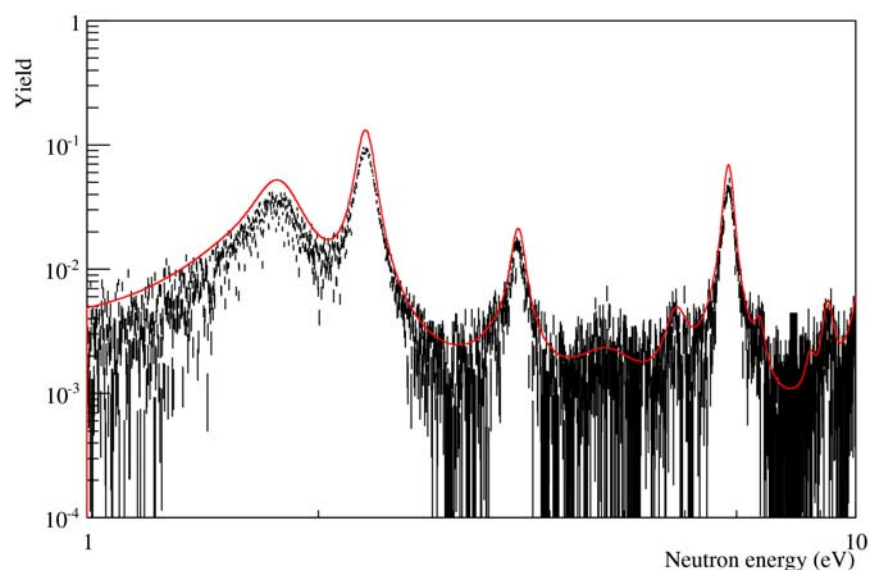
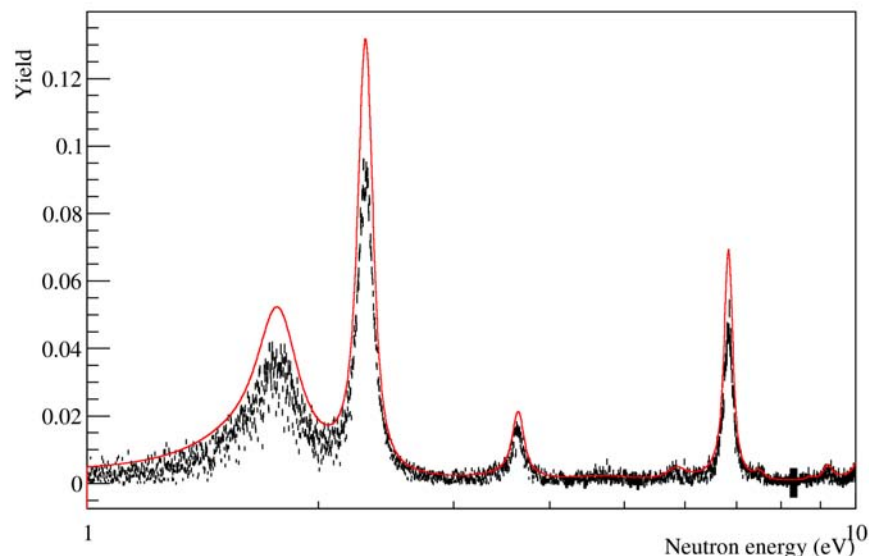


— ENDF/B-VII.1

— Yield measured at n\_TOF



# Results: Capture Yield



The neutron capture yield has been measured in the same way as the neutron induced fission yield.

The only difference lies in the event generator used in the Monte Carlo study to reproduce the neutron capture events used in the event reconstruction efficiency determination.

The agreement between the simulation and the experimental energy deposition spectrum for capture events was not the best in either tried cases.

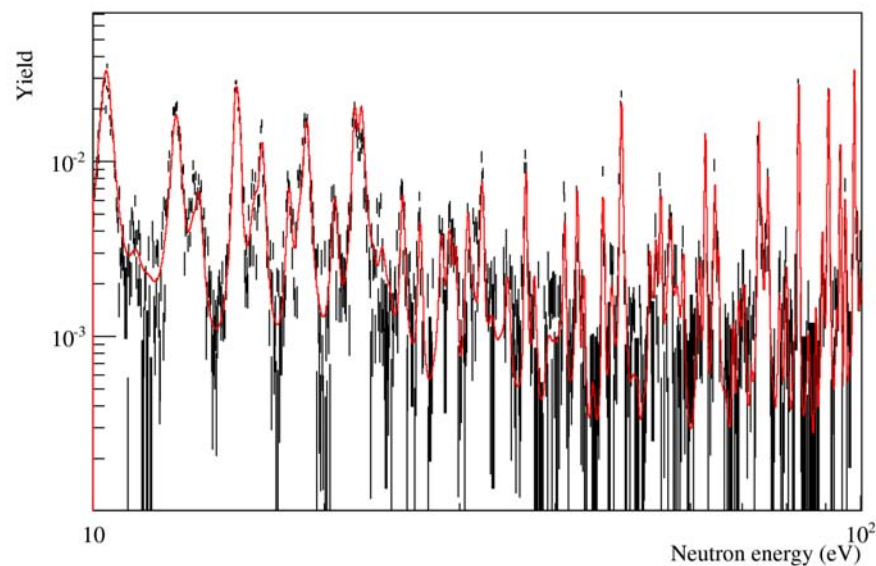
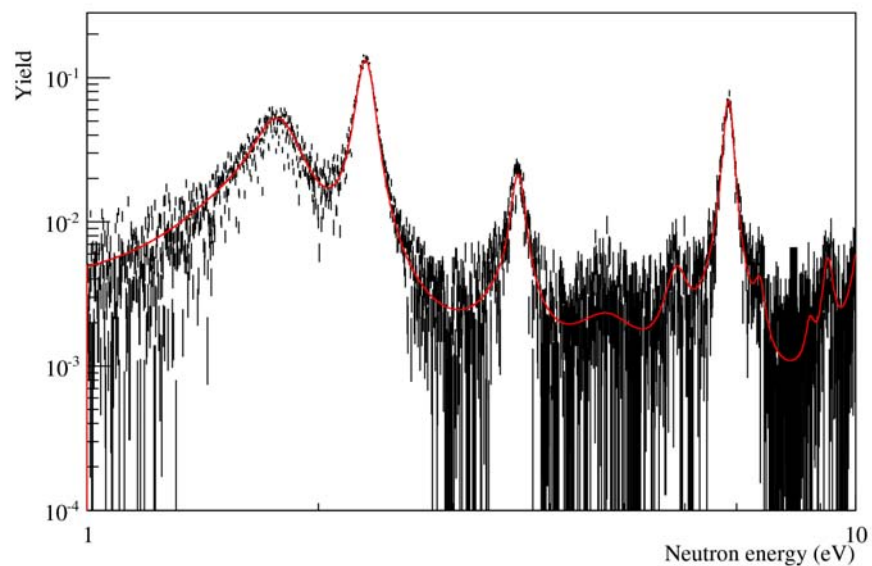
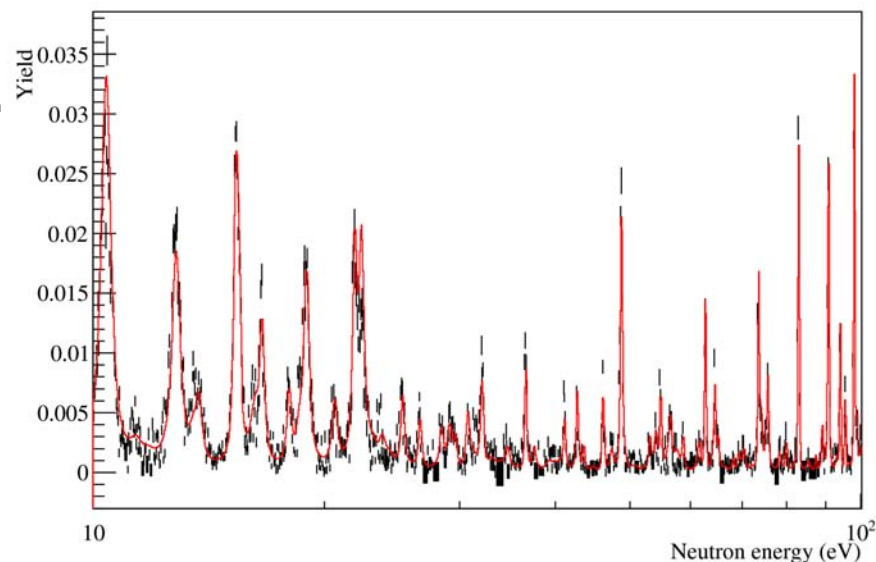
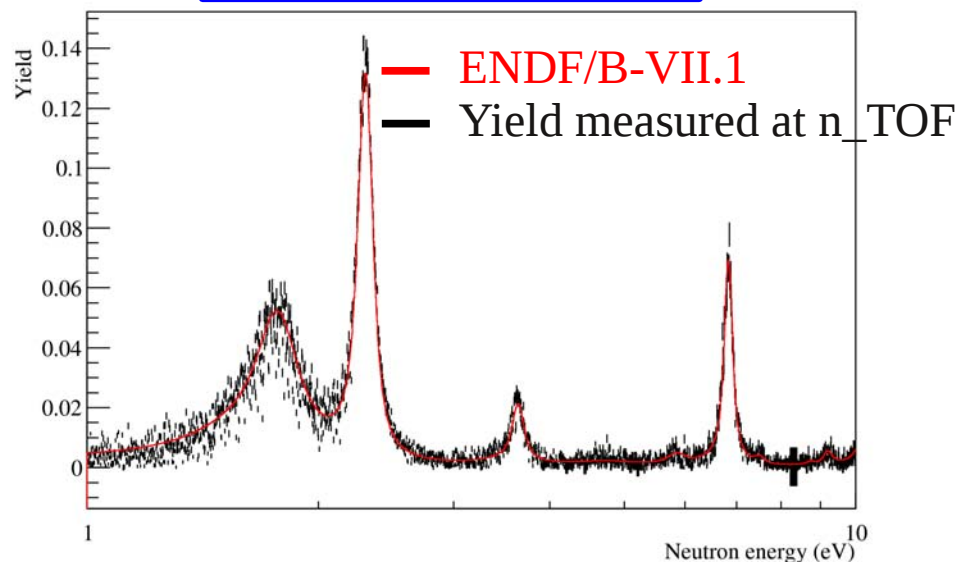
The simulations seem to point out that overall, the event reconstruction efficiency does not change dramatically with the parameterizations used.

The results show a 30% discrepancy in normalization but a good agreement in shape.

— ENDF/B-VII.1  
— Yield measured at n\_TOF

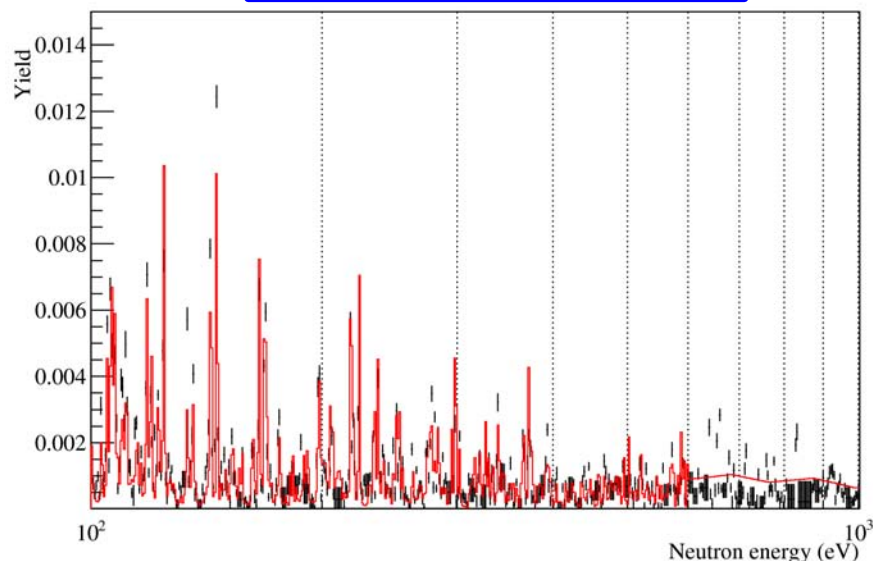
# Results: Capture Yield

Arbitrary normalization



# Results: Capture Yield

Arbitrary normalization



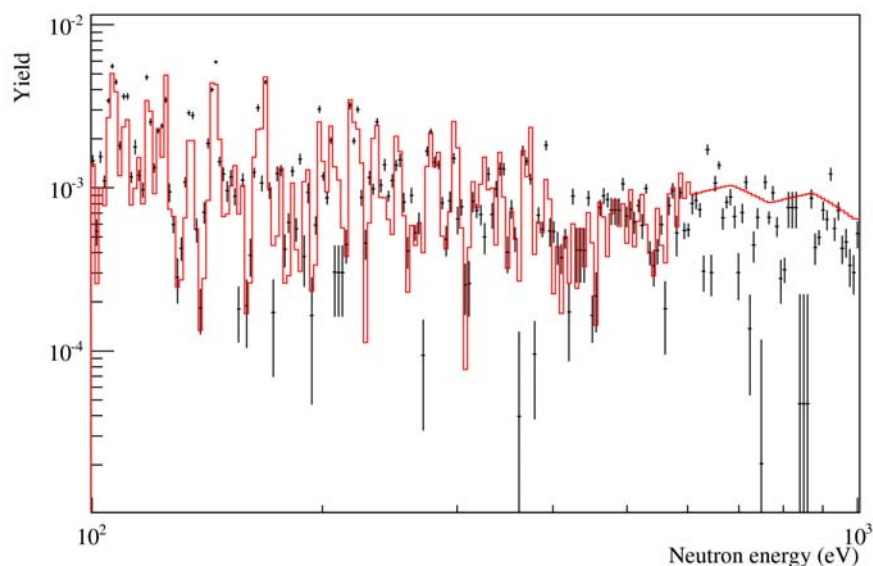
The value obtained for both capture and fission event reconstruction efficiency is very close.

This is compatible with the fact that both types of events have similar average multiplicity and energy deposition values.

The normalization was assessed to match the integral of the capture yield from the ENDF/B-VII.1 between 1 and 10 eV.

A good agreement between yield shapes is visible which validates the CSD method.

The agreement is observed over all the incident neutron energy range except beyond the resolved resonance region which ends at 600 eV.



— ENDF/B-VII.1  
— Yield measured at n\_TOF

# Uncertainties assessment

Systematic study of the uncertainty introduced by the data analysis:

- ✓ Different parameterizations for the TAC response to capture and fission
- ✓ Different deconvolution procedures.

Systematic study of the uncertainty introduced by simulations:

- ✓ Different parameterizations of the gamma generators used for determining the event reconstruction efficiency for fission and capture.

	Fission yield	Capture yield
Sample mass	5%	5%
Beam intersection	1%	1%
Flux	2%	2%
Data	2.0%	10.6%
Simulation	3%	3%
Total	6.6%	12.3%

# Conclusions

Due to the unique characteristic of the n TOF facility the measurement of the neutron capture yield of the  $^{233}\text{U}$  radioactive sample was possible with an uncertainty of 12.3% and 6.6% for the neutron induced fission yield.

The neutron capture yield was measured between 1 eV and 1 keV being the measurement limited at higher energies due to the contribution of scattering in the sample's canning and backing materials.

It must be emphasized the completely independent nature of the results obtained at n\_TOF and the agreement with the ENDF/B-VII.1 library on the neutron induced fission yield.

The same methodology was applied to the assessment of the neutron capture yield.

The results obtained and the comparisons made with the ENDF/B-VII.1 library permit to conclude that the neutron induced fission contribution was efficiently discriminated using the CSD method.

The neutron capture yield shows a disagreement of the order of 30% between the n\_TOF normalization and ENDF/B-VII.1. This cannot be attributed to the Monte Carlo modeling and can hardly be explained by the estimated 12.3% total uncertainty or with the data extraction procedure.



# Conclusions

A sizable disagreement is observed between the normalization of the neutron capture yield and the ENDF/B-VII.1 library.

Such discrepancy may be attributed to:

- Limitations in the event reconstruction efficiency methodology used in the work here presented,
- A problem in the measurements used to create the evaluation
- Or combined problems in both measurements.

Possible causes for the disagreement in the normalization may be related to the fission veto technique used in the Weston measurement used in the ENDF/B-VII.1.

Weston uses a combination of fission chamber and liquid scintillators as detection system and capture events are selected in the absence of fission fragments detected.

The problem with this technique lies in the fact that it is not possible to discriminate between fission delayed gamma emission and gammas arising from the fission neutrons interactions with the structural materials resulting in a situation where the capture contribution is difficult to assess accurately

In the n\_TOF measurement, these two components associated with fission events were considered within the scattering components used for the decomposition of the total energy spectrum.

# Future work

Certain aspects of the measurement and analysis may be improved, namely by means of:

- Performing a measurement without the titanium canning and aluminum backing.
- Gaining a better understanding of TAC's response to the delayed gamma emission associated with the fission events, would permit to have a better idea about the correctness of the neutron capture yield assessed.
- Determining the TAC's response to the neutrons produced in fission events and their interaction with the structural materials which is also a possible source of background.
- Developing a better understanding of the neutron capture deexcitation process, would provide a better description of the TAC's response to neutron capture using Monte Carlo methods and therefore a more accurate determination of the event reconstruction efficiency.
- Assessing the resonance parameter analysis to extend the accuracy of the comparison and validation of the results.
- Preparation of a “Performance Report” paper.

C. Carrapiço<sup>1, 2)</sup>, U. Abbondanno<sup>3)</sup>, G. Aerts<sup>2)</sup>, F. Álvarez-Velarde<sup>4)</sup>, S. Andriamonje<sup>2)</sup>, J. Andrzejewski<sup>5)</sup>, P. Assimakopoulou<sup>6)</sup>, L. Audouin<sup>7)</sup>, G. Badurek<sup>8)</sup>, P. Baumann<sup>9)</sup>, F. Bečvář<sup>10)</sup>, F. Belloni<sup>3)</sup>, E. Berthoumieux<sup>2)</sup>, F. Calviño<sup>11)</sup>, M. Calviani<sup>12,13)</sup>, D. Cano-Ott<sup>4)</sup>, R. Capote<sup>14,15)</sup>, P. Cennini<sup>16)</sup>, V. Chepel<sup>17)</sup>, E. Chiaveri<sup>16)</sup>, N. Colonna<sup>18)</sup>, G. Cortes<sup>19)</sup>, A. Couture<sup>20)</sup>, J. Cox<sup>20)</sup>, M. Dahlfors<sup>16)</sup>, S. David<sup>7)</sup>, I. Dillmann<sup>21)</sup>, R. Dolfini<sup>22)</sup>, C. Domingo-Pardo<sup>23)</sup>, W. Dridi<sup>2)</sup>, I. Duran<sup>24)</sup>, C. Eleftheriadis<sup>25)</sup>, M. Embid-Segura<sup>4)</sup>, L. Ferrant<sup>†,7)</sup>, A. Ferrari<sup>16)</sup>, R. Ferreira-Marques<sup>17)</sup>, L. Fitzpatrick<sup>16)</sup>, H. Fraiss-Koelbl<sup>26)</sup>, K. Fujii<sup>3)</sup>, W. Furman<sup>27)</sup>, I. Goncalves<sup>1)</sup>, E. González-Romero<sup>4)</sup>, A. Goverdovski<sup>28)</sup>, F. Gramegna<sup>12)</sup>, E. Griesmayer<sup>26)</sup>, C. Guerrero<sup>4)</sup>, F. Gunsing<sup>2)</sup>, B. Haas<sup>29)</sup>, R. Haight<sup>30)</sup>, M. Heil<sup>21)</sup>, A. Herrera-Martinez<sup>16)</sup>, M. Igashira<sup>31)</sup>, S. Isaev<sup>2)</sup>, E. Jericha<sup>8)</sup>, F. Käppeler<sup>21)</sup>, Y. Kadi<sup>16)</sup>, D. Karadimos<sup>6)</sup>, D. Karamanis<sup>6)</sup>, V. Ketlerov<sup>28,16)</sup>, M. Kerveno<sup>9)</sup>, P. Koehler<sup>32)</sup>, V. Konovalov<sup>27,16)</sup>, E. Kossionides<sup>33)</sup>, M. Krčička<sup>10)</sup>, C. Lampoudis<sup>25,2)</sup>, H. Leeb<sup>8)</sup>, A. Lindote<sup>17)</sup>, I. Lopes<sup>17)</sup>, M. Lozano<sup>15)</sup>, S. Lukic<sup>9)</sup>, J. Marganec<sup>5)</sup>, S. Marrone<sup>18)</sup>, T. Martínez<sup>4)</sup>, C. Massimi<sup>34)</sup>, P. Mastinu<sup>12)</sup>, A. Mengoni<sup>14,16)</sup>, P.M. Milazzo<sup>3)</sup>, C. Moreau<sup>3)</sup>, M. Mosconi<sup>21)</sup>, F. Neves<sup>17)</sup>, H. Oberhummer<sup>8)</sup>, S. O'Brien<sup>20)</sup>, M. Oshima<sup>35)</sup>, J. Pancin<sup>2)</sup>, C. Papachristodoulou<sup>6)</sup>, C. Papadopoulos<sup>36)</sup>, C. Paradela<sup>24)</sup>, N. Patronis<sup>6)</sup>, A. Pavlik<sup>37)</sup>, P. Pavlopoulos<sup>38)</sup>, L. Perrot<sup>2)</sup>, M.T. Pigni<sup>8)</sup>, R. Plag<sup>21)</sup>, A. Plompen<sup>39)</sup>, A. Plukis<sup>2)</sup>, A. Poch<sup>19)</sup>, J. Praena<sup>12)</sup>, C. Pretel<sup>19)</sup>, J. Quesada<sup>15)</sup>, T. Rauscher<sup>40)</sup>, R. Reifarth<sup>30)</sup>, M. Rosetti<sup>41)</sup>, C. Rubbia<sup>22)</sup>, G. Rudolf<sup>9)</sup>, P. Rullhusen<sup>39)</sup>, J. Salgado<sup>1)</sup>, L. Sarchiapone<sup>16)</sup>, R. Sarmiento<sup>1)</sup>, I. Savvidis<sup>25)</sup>, C. Stephan<sup>7)</sup>, G. Tagliente<sup>18)</sup>, J.L. Tain<sup>23)</sup>, L. Tassan-Got<sup>7)</sup>, L. Tavora<sup>1)</sup>, R. Terlizzi<sup>18)</sup>, G. Vannini<sup>34)</sup>, P. Vaz<sup>1)</sup>, A. Ventura<sup>41)</sup>, D. Villamarin<sup>4)</sup>, M.C. Vincente<sup>4)</sup>, V. Vlachoudis<sup>16)</sup>, R. Vlastou<sup>36)</sup>, F. Voss<sup>21)</sup>, S. Walter<sup>21)</sup>, H. Wendler<sup>16)</sup>, M. Wiescher<sup>20)</sup>, K. Wisshak<sup>21)</sup>, and  
The n TOF Collaboration, [www.cern.ch/ntof](http://www.cern.ch/ntof)

# Authors: Affiliation

- 1) Instituto Tecnológico e Nuclear(ITN), Instituto Superior Técnico, Universidade Técnica de Lisboa, Lisbon, Portugal
- 2) CEA/Saclay - IRFU, Gif-sur-Yvette, France
- 3) Istituto Nazionale di Fisica Nucleare, Trieste, Italy
- 4) Centro de Investigaciones Energeticas Medioambientales y Tecnologicas, Madrid, Spain
- 5) University of Lodz, Lodz, Poland
- 6) University of Ioannina, Greece
- 7) Centre National de la Recherche Scientifique/IN2P3 - IPN, Orsay, France
- 8) Atominstitut der Österreichischen Universitäten, Technische Universität Wien, Austria
- 9) Centre National de la Recherche Scientifique/IN2P3 - IReS, Strasbourg, France
- 10) Charles University, Prague, Czech Republic
- 11) Universidad Politecnica de Madrid, Spain
- 12) Istituto Nazionale di Fisica Nucleare, Laboratori Nazionali di Legnaro, Italy
- 13) Dipartimento di Fisica, Università di Padova, Italy
- 14) International Atomic Energy Agency (IAEA), Nuclear Data Section, Vienna, Austria
- 15) Universidad de Sevilla, Spain
- 16) CERN, Geneva, Switzerland
- 17) LIP - Coimbra & Departamento de Fisica da Universidade de Coimbra, Portugal
- 18) Istituto Nazionale di Fisica Nucleare, Bari, Italy
- 19) Universitat Politecnica de Catalunya, Barcelona, Spain
- 20) University of Notre Dame, Notre Dame, USA
- 21) Karlsruhe Institute of Technology (KIT), Institut für Kernphysik, Karlsruhe, Germany
- 22) Università degli Studi Pavia, Pavia, Italy
- 23) Instituto de Física Corpuscular, CSIC-Universidad de Valencia, Spain
- 24) Universidade de Santiago de Compostela, Spain
- 25) Aristotle University of Thessaloniki, Greece
- 26) Fachhochschule Wiener Neustadt, Wiener Neustadt, Austria
- 27) Joint Institute for Nuclear Research, Frank Laboratory of Neutron Physics, Dubna, Russia
- 28) Institute of Physics and Power Engineering, Kaluga region, Obninsk, Russia
- 29) Centre National de la Recherche Scientifique/IN2P3 - CENBG, Bordeaux, France
- 30) Los Alamos National Laboratory, New Mexico, USA
- 31) Tokyo Institute of Technology, Tokyo, Japan
- 32) Oak Ridge National Laboratory, Physics Division, Oak Ridge, USA
- 33) NCSR, Athens, Greece
- 34) Dipartimento di Fisica, Università di Bologna, and Sezione INFN di Bologna, Italy
- 35) Japan Atomic Energy Research Institute, Tokai-mura, Japan
- 36) National Technical University of Athens, Greece
- 37) Institut für Isotopenforschung und Kernphysik, Universität Wien, Austria
- 38) Pôle Universitaire Léonard de Vinci, Paris La Défense, France
- 39) CEC-JRC-IRMM, Geel, Belgium
- 40) Department of Physics - University of Basel, Switzerland
- 41) ENEA, Bologna, Italy